MEASURING TOTAL COLUMN WATER VAPOR BY POINTING AN INFRARED THERMOMETER AT THE SKY

by Forrest M. Mims III, Lin Hartung Chambers, and David R. Brooks

A $20 infrared thermometer pointed at the cloud-free zenith sky can measure precipitable water vapor about as well as a sun photometer, and it can do so during the day or night.

Readings from this infrared thermometer (foreground) were compared with total water vapor measured by the nearby NOAA GPS receiver at Hawaii's Mauna Loa Observatory.

Water vapor is the constituent of the atmosphere that is most responsible for weather, the hydrological cycle, and the maintenance of Earth's temperature within a range that supports life as we know it (Mockler 1995). Furthermore, water vapor condensed on sulfate and other hygroscopic aerosols can significantly increase the aerosol optical thickness of the atmosphere (Tang 1996).

The direct and indirect influence of water vapor on weather, climate, and the environment is so important that there is significant interest in techniques for inferring its vertical distribution and its total abundance in a vertical column through the atmosphere. The latter parameter, the measurement of which is the central subject of this paper, is variously described as ▶

total column water vapor, integrated water vapor (IWV), precipitable water (PW), and integrated precipitable water (IPW). Each of these phrases specifies the depth of liquid water that would result if all of the water vapor in a vertical column through the atmosphere were brought to the surface at standard temperature and pressure.

METHODS OF MEASURING PRECIPITABLE WATER. Fowle (1912) devised one of the earliest methods for measuring PW. He employed a prism spectrometer to measure the intensity of direct sunlight at the water vapor absorbing bands at 1.13 and 1.47 μm, and nearby nonabsorbing bands. Fowle's method led to the development of many kinds of spectrometers and sun photometers that measured PW, most of which employed pairs of silicon photodiodes and interference filters, one being preferentially transparent to the water vapor absorbing band at about 940 nm and the second transmitting a nearby reference band near 860 or 1,000 nm. For example, Volz (1974) developed a handheld filter sun photometer that measured PW using a pair of appropriately filtered photodiodes. Interference filters are less costly than spectrometers, but they are subject to unpredictable drift. Mims (1992) addressed this problem by developing a filterless sun photometer, which uses light-emitting diodes (LEDs) as spectrally selective photodiodes and has provided ongoing measurements of PW over south-central Texas since February 1990. Brooks et al. (2007) used LEDs in an inexpensive PW sun photometer for the GLOBE program.

Water vapor has been measured since 1930 by instrumented sounding balloons (Pettifer 2009). PW is determined by summing the mixing ratio (grams of water vapor per kilograms of dry air) as the balloon ascends. Accuracy is affected by the performance of the temperature and humidity sensors, the solar heating of these sensors, and the wake effect of the ascending balloon.

Precipitable water can also be measured by a microwave radiometer tuned to frequencies emitted by liquid and gaseous water molecules (Liljegren 1994).

Earth-orbiting satellites provide several ways to monitor water vapor. The National Oceanic and Atmospheric Administration's (NOAA's) ground-based GPS–IPW project (Gutman and Benjamin 2001) is a network across the United States and a number of other countries in which PW is inferred from the water vapor–induced delay of microwave signals transmitted by GPS satellites to ground-based receivers (Bevis et al. 1992).

Various satellite instruments are used to detect the presence of water vapor. Some observe sunlight reflected from Earth at the same near-IR wavelengths monitored by ground-based sun photometers that measure water vapor by observing direct sunlight. For example, the Moderate Resolution Imaging Spectroradiometer (MODIS) instrument aboard the *Terra* satellite measures water vapor by measuring the ratio of backscattered pairs of near-IR wavelengths (Kaufman and Gao 1992).

Another class of satellite instruments infers the presence of water vapor by monitoring the middle IR wavelengths that are emitted by water vapor that has absorbed sunlight. For example, the Television and Infrared Observation Satellite (TIROS) Operational Vertical Sounder (TOVS) on NOAA polar-orbiting satellites monitors upwelling radiation at 6.7, 7.3, and 8.3 μm to detect water vapor in the upper, middle, and lower troposphere, respectively (Soden and Lanzante 1996).

Various studies have compared the measurement accuracy and operational limitations of water vapor retrievals by sounding balloons and the ground- and space-based instruments mentioned here (Revercomb et al. 2003).

MEASURING PW WITH IR DETECTORS AND THERMOMETERS. Both clouds and water vapor absorb and re-emit radiation in discrete bands across the infrared spectrum. This permits infrared radiometers, including those configured as IR thermometers, to detect clouds, which are warmer than the clear sky, and water vapor (Sloan et al. 1955). Werner (1973) described the use of an infrared thermometer to detect clouds. The thermometer's IR sensor was a thermistor bolometer that was responsive to 9.5–11.5 μm. Today IR thermometry is used to detect the presence and temperature of clouds for

AFFILIATIONS: MIMS—Geronimo Creek Observatory, Seguin, Texas; CHAMBERS—Climate Science Branch, Science Directorate, NASA Langley Research Center, Hampton, Virginia; BROOKS—Institute for Earth Science Research and Education, Eagleville, Pennsylvania
CORRESPONDING AUTHOR: Forrest M. Mims III, 433 Twin Oak Road, Seguin, TX 78155
E-mail: forrest.mims@ieee.org

meteorological research (Morris et al. 2006). Both professional and amateur astronomers employ various IR sensors and IR thermometers to detect clouds that might interfere with their observations. For example, the Portable Cloud Sensor (Boltwood Systems Corporation) measures the sky temperature by means of a thermopile that responds to IR in a band from 8 to 14 μm (Thompson 2005).

Idso (1982) proposed the theory of measuring water vapor pressure by pointing an infrared thermometer that was sensitive to a band from 10.5 to 12.5 μm at the cloud-free zenith sky. He successfully tested his theory by conducting field tests.

Recently, Maghrabi and Clay (2010) described a method for estimating PW in a clear sky based on the ambient temperature and the signal from an IR radiometer designed for cloud detection (Maghrabi et al. 2009) that they described as a single-pixel IR detector. The detector was a thermopile with a spectral response from 6.6 to >20 μm. They compared their measurements of the cloud-free zenith sky with PW measured by a GPS receiver 30 km north of their location. From October 2002 to July 2004 their IR system provided an estimate of PW with a root-mean-square (rms) difference of 2.31 mm from the GPS PW.

Here we describe how commercially available IR thermometers (Fig. 1) can function as IR radiometers that both detect the presence of clouds and provide a means for estimating PW with an rms difference with PW given by a MICROTOPS II sun photometer of as little as 2.68 mm. This result is within 15% of

Fig. 1. The five models of IR thermometers used in the precipitable water vapor study.

that obtained by Maghrabi and Clay (2010). The IR thermometer method requires no custom electronics or expensive IR detectors and relies only on a battery-powered, handheld instrument. Nor is an ambient temperature measurement necessary, because IR thermometers incorporate temperature compensation circuitry that corrects for changes in the ambient temperature. This is usually implemented by employing a two-element detector, with one element being shielded from the source of IR being monitored and the other being exposed to the source of IR. The IR thermometer method is very inexpensive, and the second best results described below were from a $20 instrument about the size of a pocket flash memory drive (Kintrex 401).

TWO-YEAR IR THERMOMETER PW STUDY.
Geronimo Creek Observatory (GCO) is a 0.5-ha grass field in subtropical south-central Texas (29.6°N, 97.9°W) from which a series of atmospheric measurements have been made since 1990 on most days (5,489 of 7,722 days or 71.1% of available days) either at or near local solar noon. The measurement suite includes PW, solar ultraviolet (UV)-B, photosynthetic radiation, the ozone layer, and the aerosol optical depth at various wavelengths. From 8 September 2008 to 18 October 2010, the apparent temperature of the sky over GCO was measured with an infrared thermometer (Omega OS540) on 303 days (38.9% of the calendar days) when the zenith was cloud free. During this 2-yr study, the temperature at local solar noon, the usual observing time (though some measurements were made at night), ranged from 2° to 35°C, with a mean of 24.8°C. The dewpoint, which

TRIAL STUDY AT THE LANGLEY RESEARCH CENTER

A trial study was conducted at the National Aeronautics and Space Administration's (NASA's) Langley Research Center (LaRC) on 9 days during the summer of 2010. Twenty-one measurements of the temperature of the zenith sky were made by three observers using an Omega 0S543 IR thermometer. Near-simultaneous measurements of PW were made with MICROTOPS II. The data included major outliers unlike any observed during the 2-yr study and the instrument comparisons in Texas and Hawaii. These were traced to a single operator, who apparently pointed the IR thermometer at angles well away from the zenith. When the outliers were removed, the remaining data provided the expected exponential curve, an r^2 of 0.896, and an rms difference of 1 mm from PW measured by the MICROTOPS II. The LaRC experience with unskilled operators guided the development of a protocol for making consistently reliable measurements.
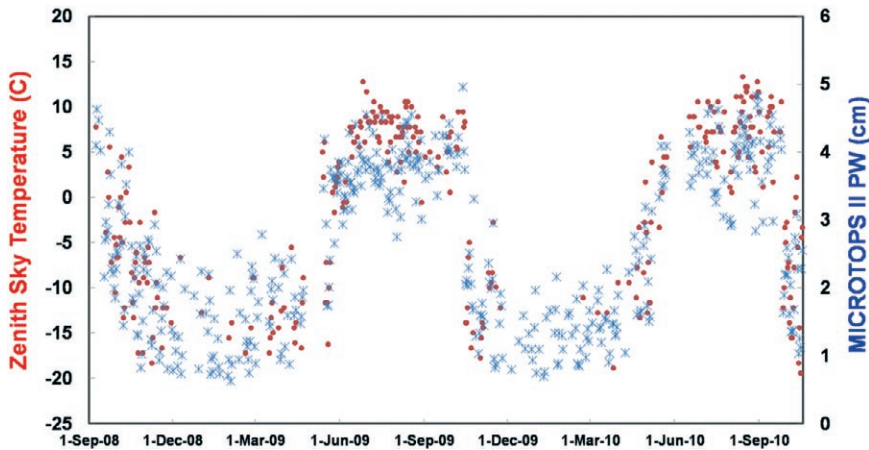
Fig. 2. A 2-yr (8 Sep 2008–18 Oct 2010) time series of the apparent temperature of the cloud-free zenith sky (Tz, red) indicated by an IR thermometer and precipitable water (PW, blue) measured by a MICROTOPS II sun photometer at Geronimo Creek Observatory, a field in south-central Texas (29.61°N, 97.93°W). This plot shows how Tz is a proxy for PW.

95% prediction bounds are from the best fits to the data provided by TableCurve 2D software (Jandel Scientific 1994), all of which are of the exponential form $y = a + b \exp(-x/c)$. In each case r^2 represents the total variance in the data that is not explained by the empirical exponential model. Note that Tz is plotted on the x axis as the independent variable instead of PW from the MICROTOPS II. This is done so that those applying the methods described herein can devise a spreadsheet in which the resulting exponential function gives PW (within the range provided by the rms difference).

is roughly correlated with PW (Reitan 1963), ranged from −12° to 25°C with a mean of 13°C.

In Fig. 2 the apparent zenith sky temperature (Tz), which is a proxy for the irradiance of the downwelling IR to which the OS540 responds, is plotted together with nearly simultaneous PW measurements that are made with a hand-held sun photometer (Solar Light MICROTOPS II; Morys et al. 2001). The lack of winter measurements is due to the minimum temperature measurement capability of the OS540. During winter, Tz often falls well below the −20°C minimum range of the OS540. The time series in Fig. 2 is ongoing and has become part of a suite of daily sun and atmospheric measurements.

Results of the 2-yr Tz study are summarized in Table 1. Figure 3 is a scattergraph of Tz measured by the IR thermometer and PW measured by MICROTOPS II during the 2-yr time series. In Fig. 3 (and also in Figs. 4, 6, and 7) and the various empirical analyses that follow, no outliers have been removed, and both day and night observations are included. The correlation coefficients (r^2), rms differences, and

The best fit to the data plotted in Fig. 3 is an exponential function that gives an r^2 of 0.90. The rms difference is 3.20 mm and the percent rms difference (rms difference/mean PW) is 10.47%. This compares favorably with the 10% error that is typically assigned to PW derived from sun photometer measurements (Holben et al. 2001). This makes the uncertainty all the more interesting because the PW standard is a sun photometer, and some of the scatter in the data likely originated from MICROTOPS II PW measurements that were found to be slightly dry with respect to GPS-derived PW measured at TXSM, the GPS receiver that
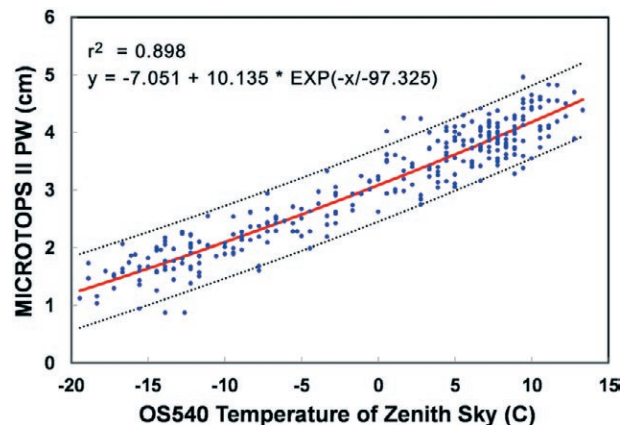

Fig. 3. Scatterplot of Tz and PW retrievals during a 2-yr study, with PW being that measured by MICROTOPS II. The best fit to the data (exponential a,b,c; red line) and the 95% prediction bounds are shown (dashed lines).

TABLE 1. Results of a 2-yr comparison of Tz and PW measured by a collocated MICROTOPS II sun photometer and a GPS receiver 31 km north-northeast.

OS540	MICROTOPS II	GPS
r^2	0.898	0.793
Rms diff	3.20 mm	5.80 mm
Rms diff/mean	10.47%	18.21%

is nearest GCO at San Marcos, Texas (TXSM), 31 km north-northeast of GCO. The mean PW measured by MICROTOPS II and GPS was, respectively, 2.93 and 3.06 cm for all days during which Tz was measured. The MICROTOPS II data might also have been biased by seasonal episodes of haze, smoke, and dust and times during which the sun was very low in the sky. GPS measurements of PW are more accurate than those by sun photometers, with an accuracy on the order of 1 mm when the required surface pressure and temperature are provided by modern surface meteorological sensors (Wolfe and Gutman 2000).

Figure 4 is a comparison of Tz and GPS-derived PW measured at TXSM. The r^2 is 0.79, and the rms difference is 5.80 mm. This rms difference is nearly twice that of the MICROTOPS II comparison and more than twice that obtained by Maghrabi and Clay (2010) in their 21-month comparison of their IR radiometer with a GPS receiver 31 km north of their site at Adelaide, South Australia, Australia, a separation distance almost identical to that between the IR thermometer measurement site at GCO and the GPS at TXSM.

As with the sun photometer comparison, various factors could have contributed to the rms differences between Tz and PW measured during the GPS comparison in Texas. For example, the comparison of IR and GPS PW by Maghrabi and Clay (2010) was made at sites with similar elevations about 10 km from the

coast, which suggests a likelihood of PW being much more similar than that at separated inland sites. This is supported by a comparison of 1 yr of PW observations at TXSM and TXAN, a nearly identical GPS site 77.5 km away at San Antonio, Texas (TXAN). While the difference of collocated GPS sites examined by Hagemann et al. (2003) is under 0.7 mm, the rms difference between TXAN and TXSM of 2.22 mm is most likely due to the elevation difference between the two stations (105 m).

A PROTOCOL FOR ESTIMATING PW FROM THE ZENITH SKY TEMPERATURE

For best results, select an IR thermometer with a minimum temperature of −60°C or less. Select a wide field of view (FOV) instrument for locations with generally clear to partly cloudy conditions. Select a narrow FOV instrument for cloudy regions.

The observer's back should face the sun, and the IR thermometer should be held in the observer's shadow to shield it from direct sunlight. When the sun is high in the sky, measurements should be made at midmorning or midafternoon. The observer should hold the instrument so that its aperture points straight up and measure Tz by closing the appropriate switch; Tz should be recorded in a notebook along with the date, Julian day, local standard time, universal time, ambient temperature, sky condition, and the operator's name. The Tz should not be measured when clouds are at the zenith.

Some IR thermometers feature an alignment laser to indicate the center of the instrument's FOV. The laser should be disabled or its aperture should be blocked with tape to prevent the beam from striking the eyes of the operator or onlookers.

An IR thermometer can be calibrated after it has collected a series of Tz measurements during a variety of conditions. Follow these steps:

1) Transfer the data to a computer spreadsheet program. If multiple people collected data, include their names or initials with their data.
2) Find the nearest NOAA GPS site (online at http://gpsmet.noaa.gov/cgi-bin/gnuplots/rti.cgi). Download the IPW for the site.
3) Enter in the spreadsheet the PW measured by the GPS closest in time (UTC) to each Tz reading.
4) Make an x–y chart in which Tz is plotted against the x axis and GPS PW is plotted against the y axis.
5) Use the spreadsheet to create an exponential fit to the points on the chart. Select the options for placing on the chart the coefficient of correlation and the equation representing the best fit to the data.
6) The equation for most spreadsheets will be of the form $y = e^x$, where x is Tz and y is PW. The typical spreadsheet exponential function is EXP(x), where x is the cell in which Tz is located. PW measured by the IR thermometer is calculated by entering the following into an empty cell: = a × EXP(b × cell), where the variables a and b are from the exponential fit to the data and "cell" is the address of the cell containing Tz. For example, the calibration function for an instrument used in this study (IRT0421) for a particular measurement was = 1.2483 × EXP(0.0241 × E286), where E286 was the cell that included Tz. This function was tested with Excel, Quattro Pro®, and OpenOffice.org spreadsheets, all of which provided the same result.
7) Finally, it is important to understand that the readout of an IR thermometer pointed at the sky indicates the magnitude of IR irradiance, which should be considered as a proxy for PW to which the device responds rather than the temperature of the sky. This calibration protocol must be performed for each instrument to compensate for their differing IR spectral responses.
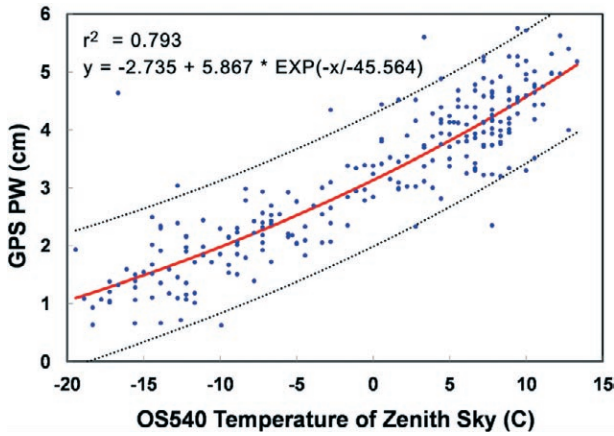
Fig. 4. Scatterplot of Tz and PW retrievals during a 2-yr study, with PW being that measured by a GPS 31 km north-northeast of the observation site. The best fit to the data (exponential *a,b,c*; red line) and the 95% prediction bounds (dashed lines) are shown.

Another possible source of uncertainty in the GPS comparisons is that while MICROTOPS II and IR thermometer measurements were made nearly simultaneously from the same site, 30-min averages of the measurements from the GPS site were posted online only twice an hour.

A better understanding of the greater difference with the GPS data awaits a follow-up study. One possibility is to collect data over an extended time with IR thermometer connected to a datalogger mounted near a GPS receiver. MICROTOPS II could be employed at intervals to provide a comparison of PW derived from it and the GPS (Bokoye et al. 2003). Simultaneous optical depth measurements by the MICROTOPS II could provide a means to evaluate the possible role of airborne dust in slightly elevating Tz.

During the 2-yr study in Figs. 2 and 3, dust originating from China (spring) and the Sahara Desert (summer) sometimes drifted over GCO, and it is possible that warming of the dust by sunlight might have caused a slight but false increase in PW derived from Tz. Major smoke and smog pollution events seem not to have significantly influenced the sky temperature. For example, when an IR thermometer was alternately pointed at the clear sky and a plume of smoke from a large grass fire, no clear difference in the temperature of the smoke plume and the sky was observed. This preliminary observation will be repeated under controlled conditions.

COMPARISON OF IR THERMOMETERS.

Twenty months into the 2-yr campaign, it became apparent that Tz was sufficiently well correlated with PW to justify expanding the study. On 17 May 2010, measurements by the OS540 were supplemented with measurements from four additional IR thermometers: Kintrex IRT0401 and IRT0421, Omega OS425, and Pro Exotics PE-3 (Table 2).

Table 2. Key manufacturer specifications of five models of commercially available IR thermometers used in the expanded study (17 May–18 Oct 2010). The last six rows give the comparison of Tz readings indicated by these thermometers and PW measured by a collocated MICROTOPS II sun photometer and GPS receivers at Mauna Loa Observatory and 31 km north-northeast of the Texas site.

Model	IRT0401	OS540	PE-3	IRT0421	OS425
Manufacturer	Kintrex	Omega	ProExotics	Kintrex	Omega
minimum *T*	−55°C (−67°F)	−20°C (−4°F)	−60°C (−76°F)	−60°C (−76°F)	−60°C (−76°F)
Accuracy	±2% or 4°F (2°C)	±2%	±2%	±1.0°C (1.8°F)	±1.0°C (1.8°F)
Distance: spot	1:1	8:1	8:1	12:1	50:1
Field of view	53.1°	7.2°	7.2°	4.8°	1.1°
Emissivity	0.95	0.95	Adjustable	0.95	Adjustable
Spectral range	5–14 μm	Unavailable	Unavailable	5–14 μm	Unavailable
MICROTOPS II: r^2	0.964	0.874	0.896	0.960	0.916
MICROTOPS II: Rms diff	2.72 mm	3.42 mm	3.82 mm	2.68 mm	2.77 mm
MICROTOPS II: Rms diff/mean	10.96%	10.47%	13.00%	10.27%	8.68%
GPS: r^2	0.944	0.824	0.807	0.936	0.881
GPS: RMS difference	4.12 mm	4.74 mm	6.26 mm	4.08 mm	3.85 mm
GPS: Rms diff/mean	15.58%	12.78%	18.41%	14.00%	10.50%

Results with both Kintrex IR thermometers were sufficiently good that the comparison was expanded with two additional IRT0401s and one IRT0421. (The data for these additional instruments were so well correlated with the originals that only the results for the original two are reported here.) The comparison of all eight of the five IR thermometer models (Table 2) was continued with 1–18 observations on each of 114 days from 17 May to 18 October 2010, including day and night observations during 10 days at Hawaii's Mauna Loa Observatory (MLO). A total of 422 sets of 2,843 individual Tz and PW observations were conducted during the campaign, with 395 sets during the day and 28 at night. Figure 5 shows scatter charts that compare four of the IR thermometers used during this study.
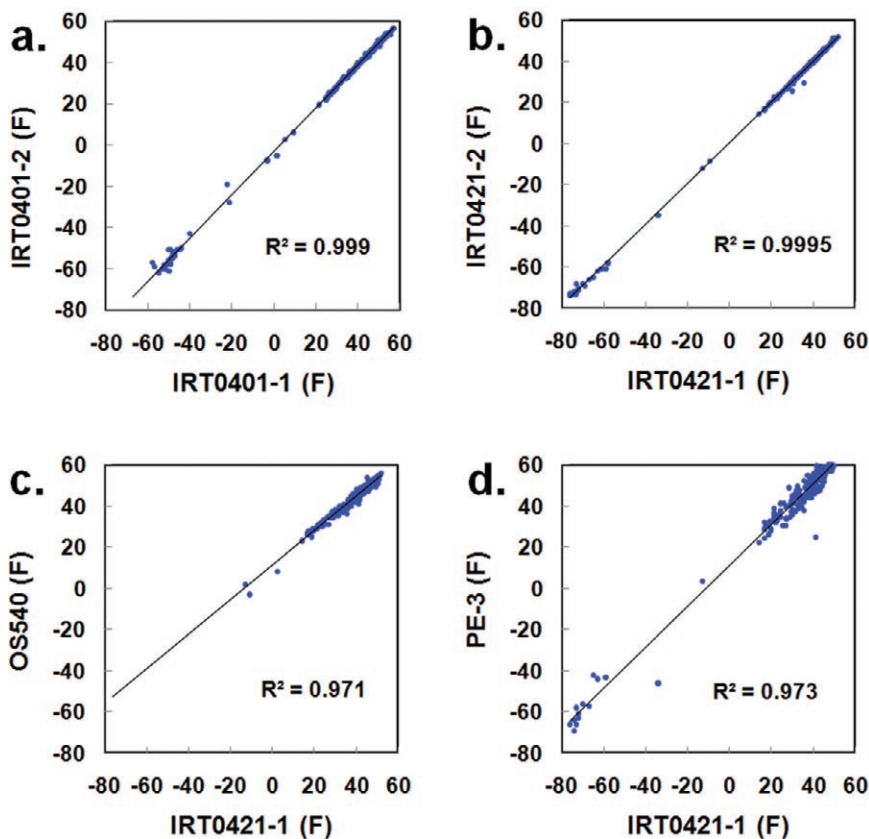

FIG. 5. Scatterplots comparing Tz measured by four IR thermometers during an expanded study from 17 May to 5 Sep 2010. The suffixes 1 and 2 indicate different versions of the same instrument model. Temperatures below −5°F were measured at the Mauna Loa Observatory, where the sky is often exceptionally dry. The temperatures were measured and presented in the Fahrenheit scale to provide higher resolution than the Celsius scale.

All but one of the IR thermometers in the study can indicate temperature in degrees Celsius or Fahrenheit within one decimal point. The exception is the Kintrex IRT0401, whose readout indicates the nearest half-degree (either degrees Celsius or Fahrenheit). Because the Fahrenheit scale has nearly twice the resolution of that of the Celsius scale, all measurements were made in Fahrenheit units. With the exception of Fig. 5, temperature scales in the plots were converted to degrees Celsius.

Some of the IR thermometers in the comparison can be adjusted to account for objects having different emissivities, while others are preset for an emissivity of 0.95, which is the value used for all measurements in this study. When set for an emissivity of 0.95, all of the instruments gave readings within 1° or 2° when pointed at various objects and the bases of overhead cumulus clouds. However, sharp differences occurred when the instruments were pointed at the open sky. This was most likely caused by differing sensitivity to water vapor resulting from the various spectral responses of the IR sensors and their optics. Unfortunately, the IR spectral response for only two of the instruments was provided by the manufacturers.

The OS425 provided the most significantly different Tz readings. This instrument was added to the study because of its very narrow field of view (FOV), which would permit it to make Tz readings when clouds are near the zenith. Most IR thermometers employ a plastic Fresnel lens to focus IR from a source onto the detector. The OS525 achieves its very narrow field of view by employing a solid convex lens that appears to be composed of germanium. The zenith sky temperature is cooler than the temperature away from the zenith because of the increasing amount of water vapor in the field of view of the instrument. Thus, the very narrow field of view of the OS425 might be responsible for some of the difference in its readings. The spectral response of the sensor and the transmission differences between plastic and germanium lenses may also have contributed to the difference.

RESULTS OF THE MULTI-INSTRUMENT COMPARISON.

No outliers were excluded from the analysis of Tz data collected during the multi-instrument study from 17 May to 18 October 2010, which are compared in the last six rows of Table 2, with PW measured by MICROTOPS II and a GPS receiver.

The Tz measured by the IR thermometers during the expanded study provided rms differences from PW measured by MICROTOPS II that ranged from 2.6 to 3.5 mm. The scatter charts in Figs. 6 and 7 show the results for two of the IR thermometers that provided some of the best results—IRT0401 and IRT0421. While both of these IR thermometers use the same detector, IRT0421 looks at a much smaller region of the sky than IRT0401. However, both these thermometers provided remarkably similar rms differences with PW measured by MICROTOPS II, with 2.72 and 2.68 mm, respectively. The exponential functions shown in Figs. 6 and 7 can be easily used to convert Tz to PW (within the rms difference).

The GPS comparisons were much less satisfactory, with the best having an rms difference from Tz of 4.04 (IRT0421) and 4.11 (IRT0401) mm. This greater difference is likely related to the distance to the GPS receiver (31 km). This will be explored during the planned study of a collocated IR thermometer and GPS receiver.

The most significant difference between the multi-instrument comparison and the 2-yr Texas study is that the minimum T that could be measured by the OS425 IR thermometer used during the latter study was only –20°C. Therefore, the 2-yr study lacks data for the coldest winter days. The IR thermometers used during the multi-instrument comparison could measure much lower temperatures (i.e., IR irradiance values), which permitted 293 measurements to be made of the very dry sky over Hawaii's MLO from 5 to 14 June 2010. These and the Texas measurements provided a very wide range of Tz such as might be expected during a full year in temperate latitudes. For example, the maximum range of Tz measured by one of the three IRT0421 thermometers was from –60.0° to +14.2° or 74.2°C. The maximum range of Tz measured by the PE-3, which required the most time to equilibrate, was from –56.1° to +21.9° or 78.0°C. These substantial ranges, which are presumably proportional to the downwelling IR, are entirely due to water vapor. As noted above, "temperature" is a proxy for the irradiance of the downwelling IR to which the instruments respond, and differences between instruments are likely due to their respective spectral responses.
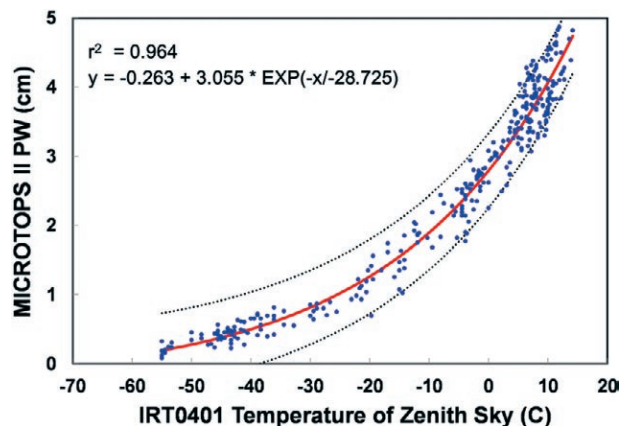

FIG. 6. Scatterplot of Tz measured by a miniature IRT0401 IR thermometer and PW measured by MICROTOPS II during the expanded study from 17 May to 18 Oct 2010. The rms difference is 2.72 mm and the rms difference from the mean PW is 10.96%. As in Figs. 3 and 4, the best fit to the data (exponential *a,b,c*; red line) and the 95% prediction bounds (dashed lines) are shown.

PW over MLO during this study was as low as 1 mm, which reduced Tz below the minimum measurement range of all of the IR thermometers. The data from a collocated GPS receiver at MLO (MLO1) suggest that the lowest PW measureable by IRT0401 and IRT0421 is, respectively, 1.8 and 3.1 mm.

The 28 sets of night Tz measurements were separately compared with PW inferred from GPS receivers. Four of the night measurements were made 37 m from a GPS receiver at MLO, and 23 were made 31 km from a GPS receiver in Texas. All of the night measurements with IRT0401 and IRT0421 fell well within the scatter of day observations and were well correlated with GPS PW (r^2 = 0.989 and 0.977, respectively).

Scans across cloud-free skies at MLO and the Texas site demonstrate that the method may be used to estimate PW by pointing the IR thermometer toward the sky at known angles away from the zenith. This method will be explored to permit measurements of PW when either the sun or clouds are near the zenith and when Tz falls below the minimum range of the IR thermometer on very cold, dry days and at alpine sites.

CONCLUSIONS.

The studies described here demonstrate that even a very inexpensive IR thermometer pointed at a cloud-free zenith sky can infer PW with accuracy comparable to that of a sun photometer. The method works during the day or night as long as the thermometer is properly used and Tz is transformed to PW by an empirical calibration algorithm based
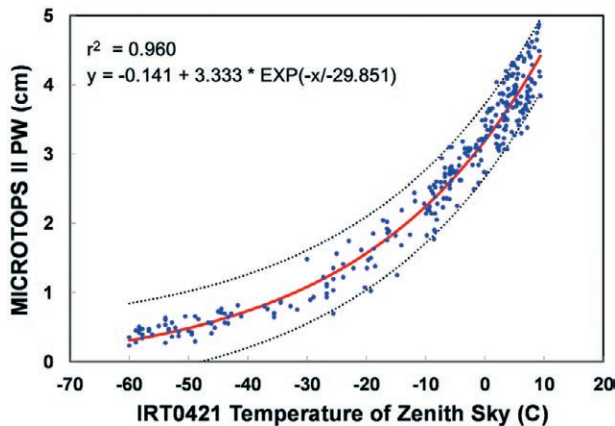
$r^2 = 0.960$
$y = -0.141 + 3.333 * EXP(-x/-29.851)$

FIG. 7. Scatterplot of Tz measured by an IRT042I IR thermometer and PW measured by MICROTOPS II during the multi-instrument comparison from 17 May to 18 Oct 2010. The rms difference is 2.68 mm and the rms difference from the mean PW is 10.27%. The best fit to the data (exponential *a,b,c*; red line) is shown.

on a reliable, independent means for measuring PW. Thus, an IR thermometer provides a very inexpensive instrument for meteorologists, cooperative weather observers, and students to measure PW and better understand the role of water vapor in weather and as the dominant greenhouse gas. While the requirement for a cloud-free zenith sky is a limitation, sun photometers are subject to a similar constraint because they require a view of the sun unobstructed by clouds.

The 2-yr observation program will be continued using the best of the IR thermometers identified during the multi-instrument comparison in 2010 to better understand any effects of smoke and dust on the readings and to identify any differences in day–night measurements. A protocol for measurements made away from the zenith will also be devised. Furthermore, it is hoped that a comparison of the IR method with a collocated GPS receiver can be arranged to develop an improved empirical PW calibration algorithm.

REFERENCES

Bevis, M., S. Businger, T. A. Herring, C. Rocken, R. A. Anthes, and R. H. Ware, 1992: GPS meteorology: Remote sensing of atmospheric water vapor using the global positioning system. *J. Geophys. Res.,* **97** (D14), 15 787–15 801.

Bokoye, A. I., A. Royer, N. T. O'Neill, P. Cliche, L. J. B. McArthur, P. M. Teillet, G. Fedosejevs, and J. M. Thériault, 2003: Multisensor analysis of integrated atmospheric water vapor over Canada and Alaska. *J. Geophys. Res.,* **108,** 4480, doi:10.1029/2002JD002721.

——, ——, P. Cliche, and N. O'Neill, 2007: Calibration of sun radiometer–based atmospheric water vapor retrievals using GPS meteorology. *J. Atmos. Oceanic Technol.,* **24,** 964–979.

Brooks, D. R., F. M. Mims, and R. Roettger, 2007: Inexpensive near-IR sun photometer for measuring total column water vapor. *J. Atmos. Oceanic Technol.,* **24,** 1268–1276.

Fowle, F. E., 1912: The spectroscopic determination of aqueous vapor. *Astrophys. J.,* **35,** 149–162.

Gutman, S., and S. Benjamin, 2001: The role of ground-based GPS meteorological observations in numerical weather modeling. *GPS Solutions,* **4,** 16–24.

Hagemann, S., L. Bengtsson, and G. Gendt, 2003: On the determination of atmospheric water vapor from GPS measurements. *J. Geophys. Res.,* **108,** 4678, doi:10.1029/2002JD003235.

Holben, B. N., and Coauthors, 2001: An emerging ground-based aerosol climatology: Aerosol optical depth from AERONET. *J. Geophys. Res.,* **106** (D11), 12 067–12 097.

Idso, S. B., 1982: Humidity measurement by infrared thermometry. *Remote Sens. Environ.,* **12,** 87–91.

Jandel Scientific, 1994: TableCurve 2D. User's manual, 391 pp.

Kaufman, Y. J., and B. C. Gao, 1992: Remote sensing of water vapor in the near IR from EOS/MODIS. *IEEE Trans. Geosci. Remote Sens.,* **30,** 871–884.

Liljegren, J. C., 1994: Two-channel microwave radiometer for observations of total column precipitable water vapor and cloud liquid water path. *Proc. Fifth Symp. on Global Change Studies,* Nashville, TN, Amer. Meteor. Soc., 262–269.

Maghrabi, A., and R. Clay, 2010: Precipitable water vapour estimation on the basis of sky temperatures measured by a single-pixel IR detector and screen temperatures under clear skies. *Meteor. Appl.,* **17,** 279–286.

——, ——, B. Dawson, and N. Wild, 2009: Design and development of a simple infrared monitor for cloud detection. *Energy Convers. Manage.,* **50,** 2732–2737.

Mims, F. M., III, 1992: Sun photometer with light-emitting diodes as spectrally selective detectors. *Appl. Opt.,* **31,** 6965–6967.

Mockler, S. B., 1995: Special report: Water vapor in the climate system. Amer. Geophys. Union. [Available online at www.eso.org/gen-fac/pubs/astclim/espas/pwv/mockler.html.]

Morris, V., C. Long, and D. Nelson, 2006: Deployment of an infrared thermometer network at the Atmospheric Radiation Measurement Program Southern Great Plains Climate Research Facility. *Proc. 16th ARM Science Team Meetin*g, Albuquerque, NM, U.S. Dept. Energy. [Available online at www.arm.gov/publications/proceedings/conf16/extended_abs/morris_vr.pdf.]

Morys, M., F. M. Mims III, S. Hagerup, S. E. Anderson, A. Baker, J. Kia, and T. Walkup, 2001: Design, calibration, and performance of MICROTOPS II handheld ozone monitor and sun photometer. *J. Geophys. Res.,* **106,** 14 573–14 582.

Pettifer, R., 2009: From observations to forecasts—Part 2. The development of in situ upper air measurements. *Weather,* **64,** 302–308.

Reitan, C. H., 1963: Surface dew point and water vapor aloft. *J. Appl. Meteor.,* **2,** 776–779.

Revercomb, H. E., and Coauthors, 2003: The ARM Program's water vapor intensive observation periods. *Bull. Amer. Meteor. Soc.,* **84,** 217–236.

Sloan, R., J. H. Shaw, and D. Williams, 1955: Infrared emission spectrum of the atmosphere. *Opt. Soc. Amer.,* **45,** 455–457.

Soden, B. J., and J. R. Lanzante, 1996: An assessment of satellite and radiosonde climatologies of upper-tropospheric water vapor. *J. Climate,* **9,** 1235–1250.

Tang, I. N., 1996: Chemical and size effects of hygroscopic aerosols on light scattering coefficients. *J. Geophys. Res.,* **101,** 19 245–19 250.

Thompson, M., cited 2005: Boltwood cloud sensor. Cloudy Nights Telescope Reviews. [Available online at www.cloudynights.com/item.php?item_id=1261.]

Volz, F. E., 1974: Economical multispectral sun photometer for measurements of aerosol extinction from .44 microns to 1.6 microns and precipitable water. *Appl. Opt.,* **13,** 1732–1733.

Werner, C., 1973: Automatic cloud cover indicator system. *J. Appl. Meteor.,* **12,** 1394–1400.

Wolfe, D. E., and S. I. Gutman, 2000: Developing an operational, surface-based, GPS, water vapor observing system for NOAA: Network design and results. *J. Atmos. Oceanic Technol.,* **17,** 426–440.